

# Plastic deformation behaviour of thermoplastic/clay nanocomposites

J.M. Gloaguen, J.M. Lefebvre

*Laboratoire Structure et Propriétés de l'Etat Solide, Université des Sciences et Technologies de Lille/CNRS, 59655 Villeneuve d'Ascq, France*

Dedicated to the memory of Roger S. Porter.

Received 1 May 2000; received in revised form 1 December 2000; accepted 6 December 2000

## Abstract

Polymer/clay nanocomposites are materials that display rather unique properties, even at low clay content, by comparison to more conventional mineral-filled polymers. Two systems are considered in the present study: the first one consists of nylon 6/clay hybrids in which in situ polymerisation is aimed at obtaining a nylon matrix strongly bonded to the delaminated clay platelets. The second one is prepared by melt dispersion of organophilic clay in polypropylene, which should in principle result in a reduced degree of polymer–clay interaction. Dynamic viscoelastic analysis is indeed indicative of a noticeable difference when referring to the molecular dynamics of the glass transition. Plasticity results, in which volume strain is recorded by video-extensometry, show extensive cavitation behaviour while retaining a fairly large strain at break, as long as deformation is performed above the glass transition temperature of the matrix. In the particular case of PA6, it is clear that the usual shear banding plastic deformation mode is altered at least in its initiation step. Localised interfacial damage promotes extensive polymer matrix fibrillation and fracture occurs predominantly in areas where delamination of the clay platelets was not fully achieved. © 2001 Elsevier Science Ltd. All rights reserved.

*Keywords:* Polymer nanocomposites; Viscoelasticity; Plasticity

## 1. Introduction

The development and characterisation of nanostructured polymer–clay composites has been a subject of raising interest in recent years (see e.g. [1,2] and references therein). These systems appear as a new class of materials, when compared to conventional filled polymers. This shows strikingly in the mechanical properties [3], but it turns out that these systems offer new perspectives in fire retardant [4] or barrier properties [5,6]. As a consequence a broad range of potential applications may be envisioned, from stiffer automotive parts, yet at lower filler content, to high barrier packaging film with insignificant loss of clarity, together with improved safety in relation to enhanced flame-retardance. Early publications have mainly dealt with polyamide 6-based nanocomposites issued from the Toyota technology which relies on in situ polymerisation of  $\epsilon$ -caprolactam in the presence of organophilic clay platelets [7]. More recent work turns towards polyolefin matrix materials with the goal of achieving clay dispersion in the melt state. It is thus a key issue in the design of these materials to monitor the dispersion of the elementary clay platelets in the polymer matrix. This involves delamination of the original layered silicate structure, as well as polymer

matrix intercalation. Clay surface cation exchange is required in order to provide organophilic cations capable of interacting with the polymer. Recent developments have primarily focused around these aspects, since with either in situ polymerisation of the polymer matrix or during melt processing, chemical modification is always required for promoting nanoscale compatibility. Local structural organisation of the nanocomposites is referred to as intercalated when some polymer material is confined in a slightly enlarged gap between elementary clay platelets whereas it is termed exfoliated when, upon in situ polymerisation or shearing in the melt state, the clay platelets have lost registry.

It is clear that from a process engineering point of view many challenging aspects still need to be addressed, but the same also holds regarding basic understanding of the elementary mechanisms operative in the observed properties. Dealing specifically with the mechanical property issue, it is possible to identify some general trends related to nanostructure organisation. When considering delaminated mineral fillers with large aspect ratio, geometrical percolation of the reinforcing elements may be considered as a reasonable assumption to account for improved mechanical response (modulus, yield stress) at low mineral

content (of the order of a few percent). The situation is, however, not optimum in all instances since thermoplastic matrix materials exhibit extremely poor sub  $T_g$  strain at break.

It is the purpose of the current study to examine the plastic deformation behaviour of nylon 6/clay and polypropylene/clay nanocomposites to gain some basic understanding on the deformation mechanisms.

## 2. Materials and experimental procedure

The first system under investigation is a nylon 6/montmorillonite clay nanocomposite, with 2% by weight mineral content, and its parent nylon matrix polymer. These are products from Ube Industries under license from Toyota. The nylon/clay hybrid is obtained by in situ polymerisation of  $\epsilon$ -caprolactam in the presence of ion-exchanged montmorillonite [7]. Reports on clay chemical modification and nanocomposite elaboration and properties may be found in the literature quoted previously [1,2].

The second materials are a PP homopolymer from Montell and a PP/clay compound prepared by melt extru-

sion of PP with 3% by weight alkyl quaternary ammonium modified Bentonite from Southern Clay Products in a rotor/stator type Kex extruder [8]. All samples have been prepared from compression moulded rectangular plaques.

Tensile testing at constant strain-rate is performed on an Instron machine, model 6025 at a crosshead speed of 5 mm/min which corresponds to a strain-rate of  $10^{-3} \text{ s}^{-1}$ . Both stress and strain are recorded, as well as volume strain [9,10]. A specific video-extensometry equipment is used for this purpose. The experimental set-up comprises the following elements:

- two CCD video cameras with zoom lenses;
- a digitising and image processing unit;
- a computer with a video interface board and three video monitors.

A specific sample geometry is used to perform the video tensile testing. It consists of a dumbbell-shaped specimen with a large radius of curvature in order to localise deformation while minimising stress triaxiality. The digitised picture of the central part of the specimen with the ink marks is processed so that the number of white pixels in all three directions is recorded as a function of time. We are thus able to obtain the true stress–strain curve and the volume strain [11].

The true stress is expressed as:  $\sigma = F/[S_0(1 + \epsilon_1)(1 + \epsilon_2)]$ , where  $S_0$  is the initial sample cross-section and  $\epsilon_{1,2}$  are the deformations in both transverse directions.

The volume strain writes:  $\Delta V/V = (1 + \epsilon_1)(1 + \epsilon_2)(1 + \epsilon_3) - 1$ , where direction 3 refers to the tensile testing axis.

Morphological studies are performed on a Field Emission Scanning Electron Microscope Hitachi S4700. Observations concern fracture surfaces as well as deformed samples viewed along the draw axis.

## 3. Results

The viscoelastic behaviour is quite revealing of the different microstructures achieved in these materials. The case of PP-based systems is examined under dynamic tension in Fig. 1a and b. The reinforcing effect of only 3% by weight of the clay is clearly displayed over the whole temperature range of evolution of  $E'$  under investigation. A 25–30% increase in stiffness is observed. The loss tangent curve in Fig. 1b shows little or no change in both the temperature position and amplitude of the relaxation peak associated with the glass transition motions around 0°C. Some differences seem to exist in the case of the crystalline relaxation beyond 50°C but though it is quite significant any comments would be too speculative at the present time and further investigations are needed. The case of the PA-based materials is considered in Fig. 2a and b. The nanocomposite

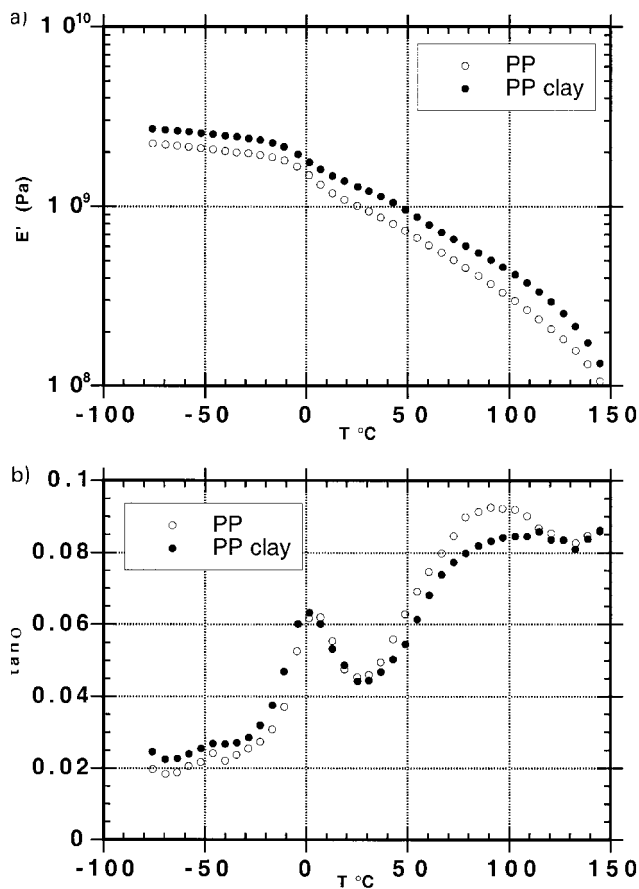


Fig. 1. (a) Tensile storage modulus at 1 Hz for the PP-based materials. (b)  $\tan \delta$  versus temperature plot for the PP-based materials.

and its parent nylon matrix have been tested in flexion. The reinforcing effect on  $E'$  is clearly more pronounced above the glass transition temperature and this may thus be indicative of a key role of mobility hindrance in the amorphous phase by the clay platelets. This assumption is supported by the reduced amplitude of the  $\tan \delta$  peak linked to the glass transition around  $50^\circ\text{C}$ , although there is no evidence for a shift of its temperature maximum. This situation of constrained dynamics has already been evoked for this particular system [3], and furthermore some clear insight regarding the change in the degree of cooperativity of chain motions in confined clay intercalated environments has been reported [12].

Returning to the present systems, comparison of Figs. 1b and 2b shows that in both cases if the position of the temperature maximum remains the same, the peak area reduction for the PA6-based nanocomposite is in contrast with the absence of any significant in the PP system. The clay platelets are expected to be bound to the polymer matrix during the in situ polymerisation of the nylon, whereas no such situation is to be encountered in the PP-based nanocomposite.

Fig. 3a and b present the room temperature tensile response of the PP-based systems. The true stress–true

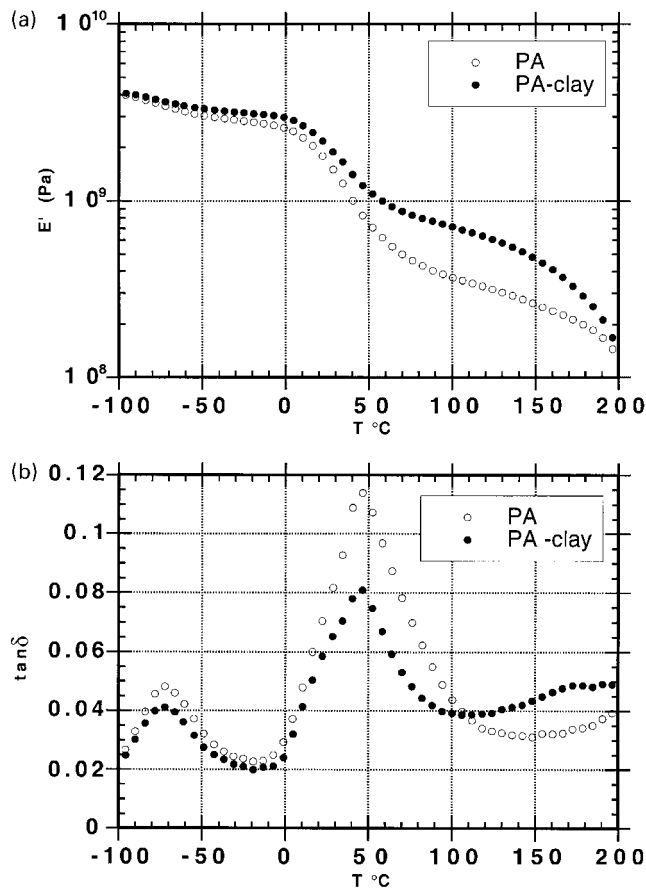


Fig. 2. (a) Flexural storage modulus at 1 Hz for the PA6-based materials. (b)  $\tan \delta$  versus temperature plot for the PA6-based materials.

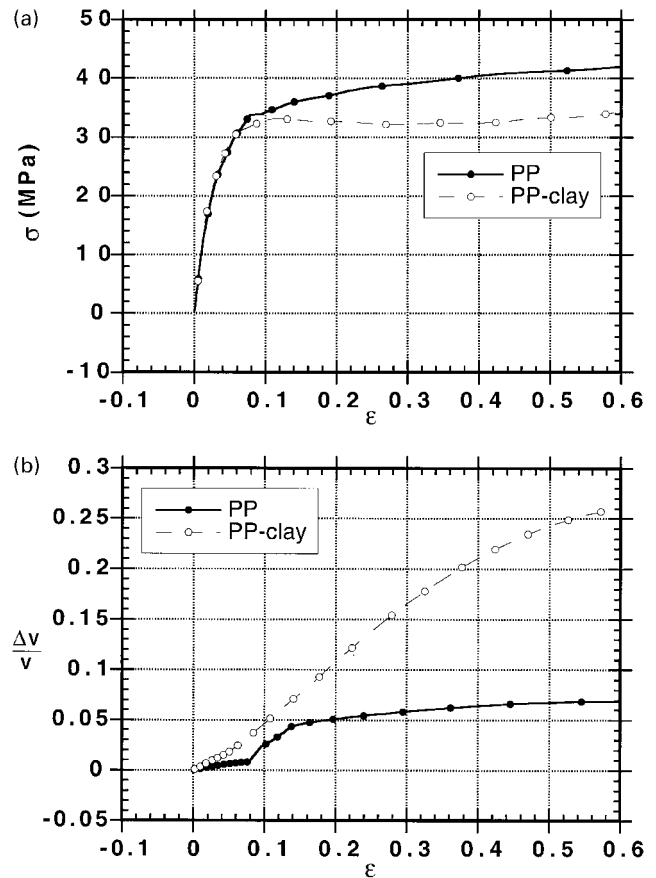


Fig. 3. (a) True stress–true strain curves at room temperature for the PP-based materials. (b) Corresponding volume strain versus elongation for the PP-based materials.

strain behaviour is indicative of a slightly reduced yield stress in the nanocomposite, although both materials exhibit a fairly large ductility. Draw temperature is situated above the glass transition temperature of the polymer matrix. The volume strain versus tensile strain plot is, however, quite revealing of a major cavitation behaviour of the nanocomposite by comparison to the PP homopolymer behaviour. The apparent sudden jump in the volume strain of the pure PP around 10% elongation is related to the development of a plastic instability (necking) in the zone of observation. A more appropriate treatment of the videoextensometry data is required in such a case but will not be considered here since it does not bring any fruitful information to the present discussion.

The data of Fig. 4 reveal the extremely fragile room temperature behaviour of the PA6 nanocomposite with a strain at break as little as 5–7%. The stress at break is of the order of 80 MPa, that is twice the yield stress of the reference PA6 material. The deformation behaviour is better compared for both systems in Fig. 5a and b above the glass transition temperature. The yield stress of the nanocomposite at  $80^\circ\text{C}$  is roughly twice as large than that of

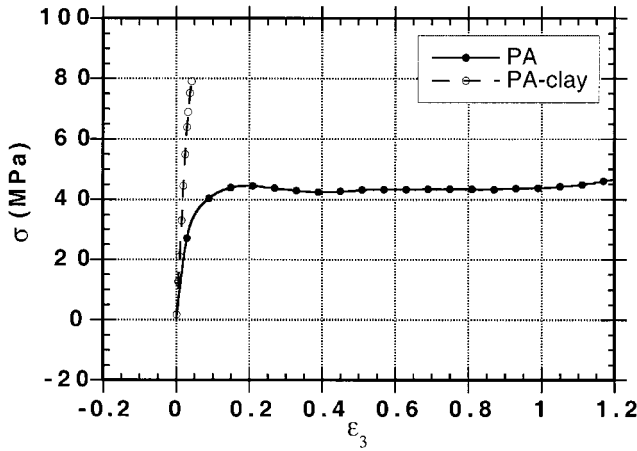


Fig. 4. Room temperature nominal stress–strain curves for the PA6-based

PA6, thus indicating that the reinforcing effect of the clay platelets is preserved when the amorphous component of PA6 is in the rubbery state. Fig. 5b illustrates the volume strain response. Owing to the significant ductility at 80°C, it is possible to take all advantages of the video-extensometry equipment in this respect. The volume strain evolution upon

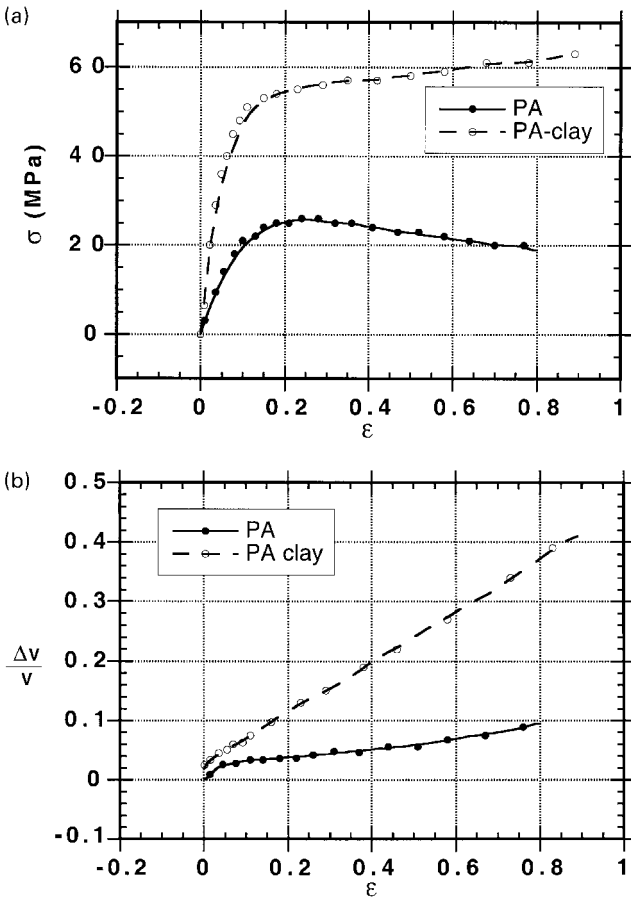


Fig. 5. (a) True stress–true strain behaviour of the PA6-based materials at 80°C. (b) Corresponding volume strain behaviour.

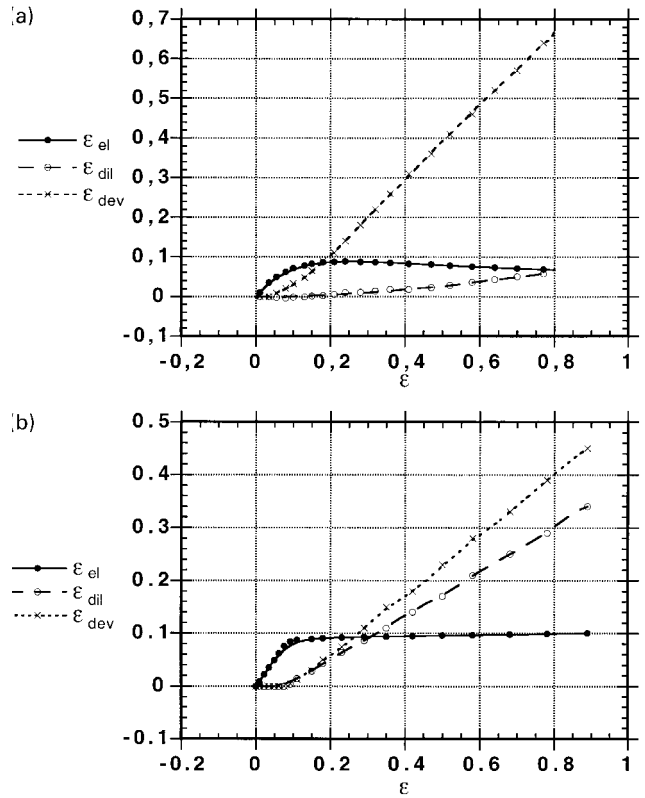


Fig. 6. (a) Contributions of the various strain components to the overall strain (PA6). (b) Contributions of the various strain components to the overall strain (Nanocomposite).

drawing is completely different, i.e. pure PA6 deforms with little volume variation, whereas the clay nanocomposite show an extensive cavitation. The observed behaviour for PA6 is in agreement with the fact that shear banding is the elementary deformation mechanism for this material. The prominent voiding in the case of the nylon/clay hybrid material is thus indicative of an important change in the response of the material.

It is worth expressing the various contributions to the overall strain, i.e. elastic, deviatoric (shear banding) and dilatational (cavitation/crazing) with the simple assumptions that shear occurs at constant volume and that cavitation and crazing strain accounts for the non-elastic volume strain [13]. According to this simple scheme, the three strain components of deformation are presented in Fig. 6a and b for the pure nylon matrix and the nylon/clay hybrid, respectively. It is clear from the data in Fig. 6a that shear banding accounts for more than 90% of the non-elastic deformation in pure nylon 6, whereas at least 45% of the latter is of cavitation nature in the nanocomposite as deduced from Fig. 6b.

#### 4. Discussion and conclusion

Cold field emission scanning electron microscopy

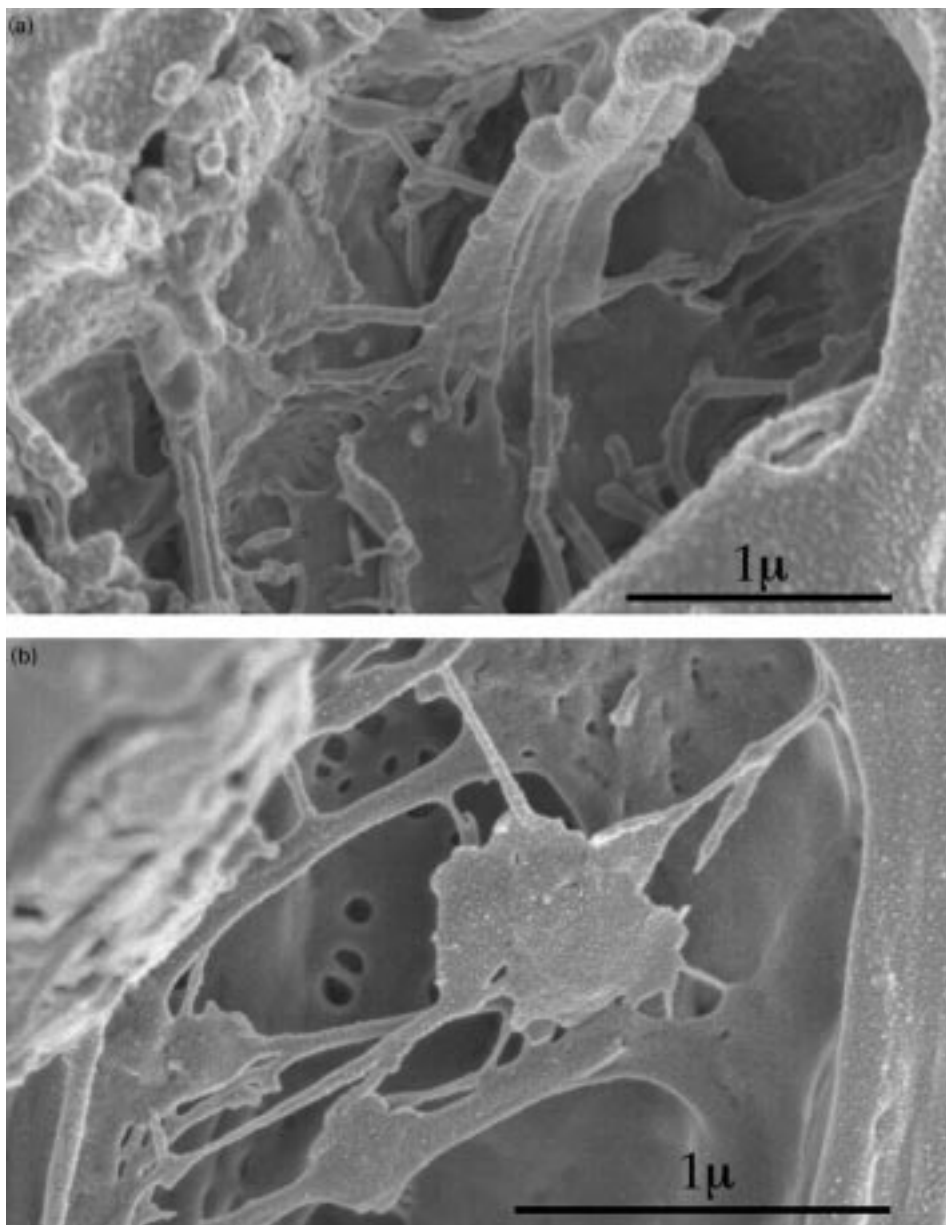


Fig. 7. SEM observation: (a) of cavitated PP-nanocomposite; (b) showing fibrillated PP-nanocomposite and polymer–clay interaction.

observations provide some qualitative indications of the microstructural evolution upon drawing. Considering first the case of the PP-based nanocomposite in Fig. 7a and b, it is clear from a fracture surface observation (a) and when viewed along the draw axis that fibrillation and cavitation is operative. Moreover, Fig. 7b shows in its central part some evidence of polymer–clay platelet (stack) interaction although no specific treatment was achieved to promote it. The identification of these clay structures in the fibrillated zones is confirmed by X-ray microanalysis which reveals the presence of Si, Al, O peaks at the specific locations of these irregular shaped platelets.

Concentrating on the case of nylon/clay hybrids, Fig. 8a

presents a typical view of the highly cavitated fibrillar structure parallel to the draw axis. Very localised damage at the polymer–mineral interface obviously induces cavitation and fibrillation much akin to profuse crazing as seen for example in High Impact Polystyrene. The extremely high surface to volume ratio of the clay mineral, and presumably strong polymer chain linkage to the mineral surface as suggested by the linear viscoelastic response is certainly able to alter noticeably the local chain dynamics. It is, however, too early to provide a clear answer as to whether some specific constrained chain conformations and/or crystalline organisation in the vicinity of the clay platelets play a role in the observed behaviour. It has yet to be confirmed if

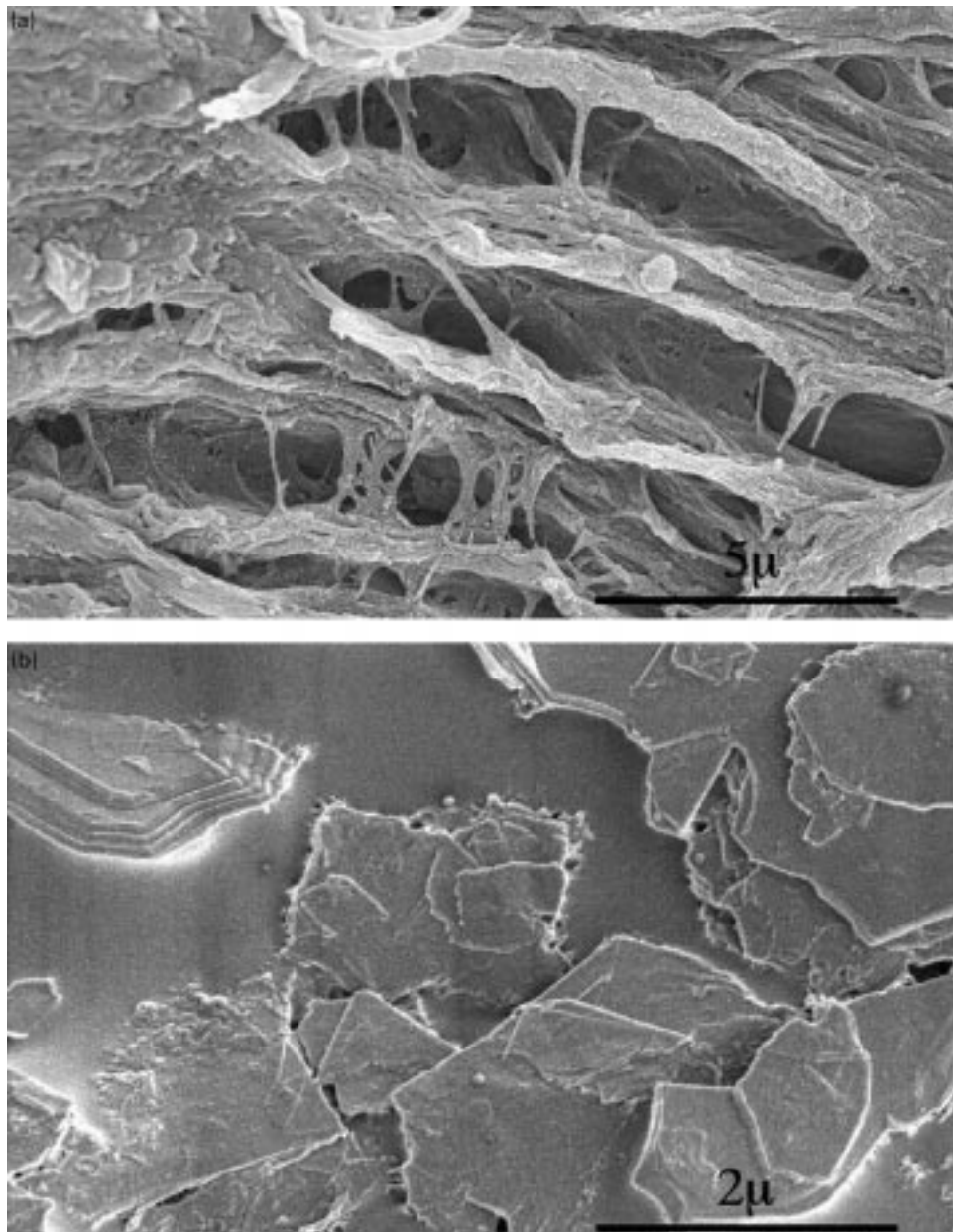


Fig. 8. SEM observation of: (a) cavitated and fibrillated nylon/clay hybrid (viewed along draw axis); (b) stacks of silicate platelets on a fracture surface.

we are dealing with very local micronecking and fibrillation or if nanoscale interfacial cavitation induces craze-like features. Nevertheless when comparing PP and PA6 nanocomposites, the largest cavitation behaviour belongs to the strongly bonded PA6 system. Dealing with microvoid formation, an interesting suggestion is provided by Michler and coworkers [14] in their work on PA12-based nanocomposites where they attribute a specific role to stacked silicate layers, depending on their orientation with respect to the tensile axis. In this scheme, splitting of intercalated structures ought to promote microcavitation rather than plastic shear and this would contribute to the development of the observed damaged structure. Fig. 8b shows an example of a typical fracture surface where stacks of clay plate-

lets obviously badly dispersed have induced local breakage. This is indeed consistent with the suggestion evoked above.

Whether toughness may be brought by this kind of reinforcement has yet to be proved but it is quite clear that major improvements rely on the quality of nanocomposite elaboration and processing. Polymer–clay nanocomposites propose challenging questions regarding the fundamental aspects of the deformation mechanisms, both with respect to the local polymer dynamics and to the scale of initial interfacial damage and local matrix ligament thickness. These parameters may alter the classical response of a given polymer matrix. From an experimental point of view, video-extensometry appears as an interesting tool to evaluate the changes induced in these materials upon drawing.

Nanoscale observations are now needed in order to elucidate the microstructural evolution as a function of strain.

### Acknowledgements

Financial support from Région Nord-Pas de Calais and European fund FEDER, for developing the Scanning Electron Microscopy is gratefully acknowledged. Thanks are expressed to J. Gilman and T. Kashiwagi from NIST for making the nylon 6/clay hybrid materials available to the polymer group in Lille.

### References

- [1] Giannelis EP, Krishnamoorti R, Manias E. *Adv Polym Sci* 1999;138:107.
- [2] Alexandre M, Dubois P. *Mater Sci Engng* 2000;28:1.
- [3] Kojima Y, Usuki A, Kawasumi M, Okada A, Fukushima Y, Kurauchi T, Kamigaito O. *J Mater Res* 1993;8:1185.
- [4] Gilman JW. *Appl Clay Sci* 1999;15:31.
- [5] Yano K, Usuki A, Okada A, Kurauchi T, Kamigaito O. *J Polym Sci, Polym Chem Ed* 1993;31:2493.
- [6] Messersmith PB, Giannelis EP. *J Polym Sci, Polym Chem Ed* 1995;33:1047.
- [7] Usuki A, Kawasumi M, Kojima Y, Okada A, Kurauchi T, Kamigaito O. *J Mater Res* 1993;8:1174.
- [8] KEX system from Draiswerke, Mannheim, Germany.
- [9] Bucknall CB. *Toughened plastics*. London: Applied Science, 1995.
- [10] Yee AF, Pearson RA. *J Mater Sci* 1986;21:2462.
- [11] François P, Gloaguen JM, Hue B, Lefebvre JM. *J Phys III, France* 1994;4:321.
- [12] Vaia RA, Sauer BB, Tse OK, Giannelis EP. *J Polym Sci, Polym Phys Ed* 1997;35:59.
- [13] Heikens D, Sjoerdsma S, Coumans WJ. *J Mater Sci* 1981;16:429.
- [14] Kim GM, Michler GH, Reichert P, Kressler J, Mülhaupt R. *Polym Mater Sci Engng* 1998;79:178.